Making negatives and plates for printing by electroerosion: II. Larger-scale fabrication and testing

by M. S. Cohen A. Afzali

E. E. Simonyi

M. Desai

K. S. Pennington

The principles of producing direct negatives and direct plates by electroerosion writing were given in Part I of the present series of papers. Part II is concerned with larger-scale fabrication techniques, characterization methods, and the results of tests, together with their interpretation. Major problems which were encountered are also presented with their solutions. Sheet material for the direct negative/direct plate (DNP) was made by 1) Coating polyester rolls with an underlayer. The underlayer coating fluid contained silica, a cellulosic binder, a saturated polyester dispersant, and an isocyanate cross-linker. The coating fluid was carefully milled to control silica particle size before coating.

2) Curing the rolls either at ambient or elevated temperature. 3) Calendering the underlayer. 4) Vacuum-depositing an aluminum film. 5) Coating with an overlayer containing graphite and a binder. Maintenance of good control of material characteristics was found essential for acceptable functional performance. Among the parameters requiring control were underlayer thickness and surface roughness, aluminum thickness, and overlayer thickness, as well as the composition of the various components. After fabrication, functional testing of the DNP material was carried out on the IBM 4250 printer in order to study the major performance problems of scratching, writing failure, head wear, gouging,

Copyright 1991 by International Business Machines Corporation. Copying in printed form for private use is permitted without payment of royalty provided that (1) each reproduction is done without alteration and (2) the *Journal* reference and IBM copyright notice are included on the first page. The title and abstract, but no other portions, of this paper may be copied or distributed royalty free without further permission by computer-based and other information-service systems. Permission to *republish* any other portion of this paper must be obtained from the Editor.

and head fouling. Scratching could be suppressed by decreasing the surface roughness and increasing the thickness of the overlayer. Writing efficiency could be improved by increasing the roughness, decreasing the overlayer thickness, decreasing the aluminum thickness, and increasing the pulse length. Head wear could be suppressed by calendering and reducing the roughness. Gouging and excessive head wear could be suppressed by adequate milling, dispersing and filtering of the underlayer coating fluid. and calendering and curing of the coated web. while ensuring good underlayer-substrate adhesion. Fouling was reduced by decreasing the overlayer thickness and reducing the writing pulse length.

1. Introduction

The fundamental physical principles and operational behavior of the direct negative/direct plate (DNP) were explored in Part I of the present series of papers. In the present paper, Part II, practical procedures for larger-scale fabrication of these materials are discussed, along with measurements appropriate for their characterization. The major problems which had to be solved for the practical realization of this new technology are also presented. During the course of the present studies, additional insights were gained into connections between material constitution and behavior under functional test; these new insights are discussed.

In the present work the emphasis was not on laboratoryscale samples, as in Part I, but rather on fabrication of rolls of DNP material on a scale which was designed to demonstrate production feasibility. For this purpose, rolls of polyester film were used for the substrate. First the underlayer was applied by web-coating techniques, then the aluminum layer was deposited in a web-fed vacuum metallizer, and finally the overlayer was applied, again by web-coating techniques. The width and length of the web in the primary "master" rolls were determined by the capabilities of the particular web coater used; typical master rolls contained a web about 35 cm wide and 900 m long. After the three layers were applied, the master rolls were slit and rewound into small rolls suitable for use with the IBM 4250 electroerosion printer; typically these were about 26 cm wide and 100 m long.

The DNP material described here must simultaneously meet the requirements for acceptable performance on the IBM 4250 printer and provide satisfactory service as a direct negative and a direct plate. These goals were

Web-coating facilities under the direction of D. W. Carlsen of IBM Boulder were used for these experiments.

achieved by careful control of fabrication processes and careful monitoring of material characteristics at each stage of fabrication. After a discussion of the latter topics, the problems encountered with use of the DNP material on the 4250 printer are presented. The additional problems associated with use as a direct negative and direct plate are discussed in Part III, along with pressroom procedures which were found to be beneficial.

The reader is referred to Part I for a more complete introduction to the basic structure and usage of direct negatives and plates.

2. Fabrication processes and controls

The polyester substrate was coated sequentially with the underlayer, the aluminum film, and the overlayer.

• Substrate

A clear polyester substrate was used. The thickness of this substrate was chosen to be 100 μ m as a compromise between the mechanical flexibility required for reliable operation of the IBM 4250 printer and the mechanical strength needed for pressroom operations. A grade of polyester film having high optical transmission and low haze characteristics was chosen.

The adhesion of the underlayer to the polyester substrate was found important, as is discussed in more detail below. Very poor underlayer adhesion resulted if an untreated polyester substrate was used, as was confirmed with simple peel tests with pressure-sensitive adhesive tape. However, if the material was subsequently subjected to a cure treatment, say 75-100°C for 24 h, a marked improvement in adhesion resulted. It was also found that subjection of the polyester to a corona-discharge treatment prior to application of the underlayer could improve adhesion. However, the most practical method of ensuring good adhesion was found in a third alternative, namely the use of polyester film precoated with a very thin primer designed to offer improved adhesion. (Such a primercoated polyester film is Hostaphan 4500, American Hoechst Corp., Wilmington, DE.)

Underlayer

As previously described in Part I, a thin hard underlayer is required with a prescribed surface roughness in order to obtain good performance during writing with the IBM 4250 printer. A hard underlayer was subsequently also found beneficial in obtaining longer press life for the direct plate (Part III). To obtain such an underlayer, silica particles were dispersed in a cellulosic binder which was mixed with an isocyanate cross-linker; this material was then coated on the polyester substrate.

The underlayer fabrication process may be divided into three major operations:

• Preparation of the coating fluid.

- The coating operation.
- Postcoating operations involving curing and calendering.

Preparation of the coating fluid

The standard method for making a well dispersed coating fluid [1] involves as a first step the formulation of a concentrated "mill base" mixture of pigments, binder, and other agents, which is subjected to mechanical milling action. When the milling is completed, a "let-down" of the mill base is carried out, at which time the mill base is diluted and other components are mixed in prior to the coating process.

In the present case the pigment chosen was natural silica particles. This material was selected because when coated on the substrate in a thin layer in a suitable binder, the required hardness and surface roughness could be attained. Furthermore, the refractive index of the silica closely matched that of the binder, so that light scattering was minimized. The binder chosen was cellulose acetate butyrate (CAB), which was selected because its high density of hydroxyl groups permits good cross-linking, while it is easily soluble in common solvents. A saturated polyester was also added as a dispersant; a thin layer of this polyester is thought to coat each silica particle, thereby providing better bonding to the CAB matrix. Isocyanate was chosen as the cross-linking agent. Other components added in very small proportions were a flowpromoting agent and polytetrafluoroethylene particles, which aided the milling operation and may help suppress fouling (see below).

Formulation A² for underlayer coating fluid is given in detail in Table 1. A solution of CAB in a mixture of about 9:1 tetrahydrofuran (or methyl ethyl ketone) and toluene was first made in a high-speed stirrer. Next a mill-base mixture was made of CAB solution, silica, polyester, polytetrafluoroethylene, and surfactant. After stirring, this mill base was subjected to a milling operation to reduce the particle size while obtaining a good dispersion.

The milling operations were carried out with a media mill [1]. The milling conditions and milling time had to be controlled very carefully because the resulting surface roughness of the underlayer was found to decrease monotonically with increasing milling time.

After the milling operation was completed, the mill base was removed from the mill and a let-down mixture was prepared. In this step, the additional CAB solution, the isocyanate cross-linker, the flow-promoting agent, and the catalyst were added, while more solvent was added to reduce the viscosity to a value required for coating.

An eight-hour "pot life" was found for this coating fluid; i.e., the coating fluid had to be used within 8 h of its preparation in order to avoid gelation.

Table 1 Coating liquid for underlayer: Formulation A.

Component	Description	Parts by weight
Mill base		
22% CAB solution		54.58
Silica (particles):	Imsil A 108	3.35
Silica (particles):	Imsil BP5	6.47
Saturated polyester:	Multron R221-75	0.49
Polytetrafluoroethylene	du Pont Teflon®	
(particles):	DLX-6000	0.49
Let-down Mill base listed above Isocyanate cross-linker: Solvent: Solvent: Flow agent:	Mondur CB-75 Tetrahydrofuran Toluene FC-430	12.01 20.35 2.19 0.06
22% CAB solution		
Solvent:	Tetrahydrofuran	70.15
Solvent:	Toluene	7.84
Cellulose acetate	Eastman CAB	
butyrate:	553-0.4	22.00

- $PVC SiO_2 = 17.1\%$; PVC polytetrafluoroethylene = 0.98%
- Saturated polyester is 1.72% of nonpigment solids, or 3.06% of CAB.
- CAB 553.4, Eastman Chemical Products, Kingsport, TN. Imsil A108, Imsil BP5, Illinois Mineral Corp., Cairo, IL
- Multron R221-75, Mobay Chemical Corp., Pittsburgh, PA
- Teflon DLX-6000, E. I. du Pont de Nemours & Co., Wilmington, DE.
- Mondur CB75, Mobay Chemical Corp., Pittsburgh, PA.
- FC-430, 3M Corp., St. Paul, MN.
- 9. Methyl ethyl ketone could be substituted for tetrahydrofuran.

Reproducibility of the coating-fluid chemistry was aided by careful attention to the various weighing, mixing, and milling operations involved in the preparation of the underlayer coating fluid. It was also helpful to have a rough independent check on the milling action; such a check was obtained by measuring viscosity. For the web coater used in the present experiments, good results were obtained when the coating-fluid viscosity was in the range of 0.16-0.18 Pa-s.

Coating operation

After the coating fluid was prepared, it was brought to the coating unit. This machine consisted of a motor-driven web-transport mechanism which fed the web at a controlled speed and tension past a coating head, then through an oven and into a rewind station. The coating fluid was pumped to the "hydropneumatic" coating head [2] through a filter. [Typically a 40-μm filter was used (Pall Trincor Corp., Vauxall, NJ).] By proper control of the flow rate of the coating fluid and the web-transport speed (typically 30 m/min), and by correctly setting the coatinghead controls, the coating thickness and width (relative to the web width) could be controlled. The dried underlayer thickness was usually 5-7 μ m as checked by a micrometer.

Immediately after coating, the web passed through an oven chamber through which hot air was forced at high speed. The residence time in the oven was typically about

² Alternative Formulation B is discussed in Section 5.

Table 2 Coating liquid for overlayer.

Component	Description	Parts by weight
Hydroxyethylcellulose:	Hercules Natrosol	0.174
Graphite dispersion:	Acheson Dag 191	5.340
Cross-linker:	du Pont Tyzor LA	0.051
Water:	•	94.435

- 1. Coating liquid makes a solution with 1% solids
- Natrosol, Hercules Inc., Wilmington, DE (added in form of a 2% solution in water).
- 3. Dag 191, Acheson Colloids Co., Port Huron, MI (15% solids)
- Tyzor LA, E. I. du Pont de Nemours & Co., Wilmington, DE (lactic acid titanium chelate; 50% solution in water).

one minute at a temperature of about 90°C. Under these drying conditions negligible residual solvent was found in the underlayer. [Two techniques were used to check for residual solvent content: 1) The weight loss during a prolonged high-temperature anneal (>100°C) was studied. 2) Gas chromatography was used to study gases evolved during high-temperature anneal (>100°C). Neither technique showed residual solvent within measurement error, which was a few parts per million in the gas chromatography study.]

Postcoating operations

Under certain circumstances it was found advantageous to subject a master roll to a high-temperature cure treatment, as discussed below. For this purpose the wound roll was placed in an oven which was kept at a constant temperature using recirculating forced hot air. The cure treatment was more effective as the temperature increased, but practical difficulties were found to limit the maximum usable temperature to 50–75°C for two reasons: 1) Too high a temperature caused "blocking," i.e., adhesion of one wind of a master roll to its neighbor. (When such blocking occurred, it was not in the coated regions but in the uncoated margins; i.e., the prime coatings on the juxtaposed winds adhered to one another.) 2) Too high a temperature caused distortion of the polyester substrate.

Another postcoating operation which was found to be indispensable for good characteristics was a calendering treatment. After curing, the master roll was fed through a calender having two operational nips in which a highly polished steel roller rotated against a softer nonmetallic backing roller. Typical linear pressures used in the nip were roughly 3×10^5 N/m, where the pressure is measured in force per unit length of the roller; typical temperatures were about 85°C, and web speeds of roughly 150 m/min were used.

Aluminum layer

After application of the underlayer, the aluminum film was deposited in a vacuum metallizer designed for web

coating.3 Such machines are fitted with an unwind and a rewind station in the vacuum so that the web can be moved at constant tension and high speed (typically 60-80 m/min) past an array of resistance-heated evaporation sources. By controlling the relative temperatures of the sources and the speed of the web, the film thickness can be kept constant across both the width and length of the web. Continuous electrical resistivity and transmission optical density measurements made during deposition can be used to monitor the aluminum thickness; in practice, control of the optical density was given priority over the electrical resistivity. (It may be noted that in the present application such measurements were both easier to make and more meaningful than the "thickness" measurements made for small laboratory vacuum-deposition systems, which are typically carried out with quartz-crystal rate monitors or with post-deposition profilometer measurements.)

Overlayer

After deposition of the aluminum film, the lubricating overlayer was applied. For this purpose a water dispersion of graphite was mixed into a solution of 2% hydroxyethylcellulose (HEC) in water with a high-speed stirrer. A very high dilution in water was necessary in order to permit controlled coating of the extremely thin overlayer; the resulting thick liquid film applied during the coating also helped prevent scratching of the underlying aluminum layer by the coating head. It was also found that subjecting the overlayer coating fluid to high-shear stirring to break up agglomerates, followed by fine-pored filtration, helped produce a uniform, streak-free overlayer.

The complete coating-fluid formulation is given in **Table 2**. The HEC served as an additional binder for the graphite lubricant, while the titanate cross-linker was added to help prevent rub-off of the overlayer during handling.

Binders other than HEC have been investigated, notably polyvinyl ethyl ether maleic anhydride (available from GAF Corp., New York, NY, under the trade name Gantrez). In addition to these water-based systems, solvent-based overlayer systems have also been studied; e.g., a solvent-based graphite dispersion⁵ was used with CAB as an added binder. Such alternative solvent-based formulations showed functional performance on the IBM 4250 printer equivalent to that of the formulation of Table 2. The water-based formulation was preferred because of the avoidance of solvent-disposal problems, and because the associated hydrophilicity of the overlayer is advantageous for the direct-plate application (Part II).

³ Such vacuum metallizations were performed under the direction of D. Parker at IBM Lexington and by Vacuum Depositing Inc., Louisville, KY.

⁴ The overlayer coating fluid was passed through a 5-μm filter (Pall Trincor Corp., Vauxall, NJ) placed just before the coating head. T. J. Marsh of IBM Boulder studied the relationship between overlayer uniformity and dispersion and filtering of the coating fluid.

⁵ Dag 154, Acheson Colloid Corp., Port Huron, MI.

The same coating unit which was used for application of the underlayer was also used for the overlayer, and the coating procedures which were employed were similar to those used for the underlayer. However, the mode of coating was changed from that used for the underlayer in that the thickness of the overlayer was determined by metering the coating-fluid flow to the coater head. The dried overlayer thickness could thus be calculated from the web speed, the known concentration of the coating fluid, and the speed of the pump which controlled the flow rate of the coating fluid. For effective control of the very thin overlayer (areal density of about $3 \mu g/cm^2$), a very dilute coating fluid was required (about 1% solids).

3. Control of material characteristics

The characteristics of the DNP material had to be checked at each step of the fabrication process in order to maintain good final functional quality. The parameters which had to be monitored, along with the corresponding measurement techniques, have been mentioned above. This subject is explored more fully in this section.

• Underlayer morphology

The morphology of the underlayer is one of the most critical factors in determining operational behavior, and must be controlled carefully.

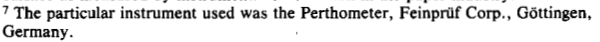
Measuring underlayer morphology

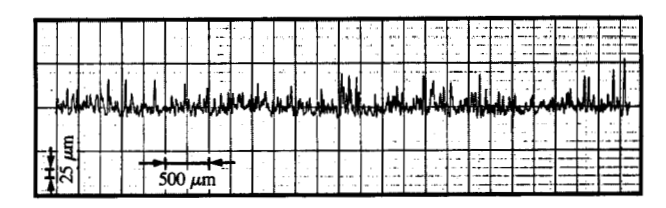
It was found that the most reliable indication of the attainment of the desired specifications for surface morphology came from direct measurements of the completed underlayer. Accurate and reproducible surface-morphology characterization was achieved by use of a profilometer. In this instrument a sharp metal tip is dragged across the surface, and the excursions corresponding to surface variations are recorded and analyzed with a microprocessor. A typical trace obtained with such an instrument is shown in Figure 1.

Profilometers⁷ offer a selection of different mathematical averages of the surface profile [3]. The parameters which were explored for the present application are R_a , R_z , and t_{p50} . Here R_a is the mean, taken over the measuring length, of the absolute value of the deviations from the reference line (the average vertical displacement). The parameter R_z represents the mean of the maximum peak-to-valley distances for five successive sampling lengths. The parameter t_{p50} is related to the concept of the bearing ratio; this concept is meaningful in the present case because it may be associated with the contact geometry between a

⁶ Less satisfactory characterizations of the surface morphology were obtained by measurements of oblique-incidence optical reflectivity as measured by a "glossmeter," or by the resistance to a restricted air stream directed parallel to the surface as measured by instrumentation common in the paper industry.

The particular instrument used was the Perthometer Feinproff Corp. Göttingen





Flaure *

Profilometer trace of master roll C1503 (before calendering). R_a = 0.420 μ m, R_z = 3.33 μ m.

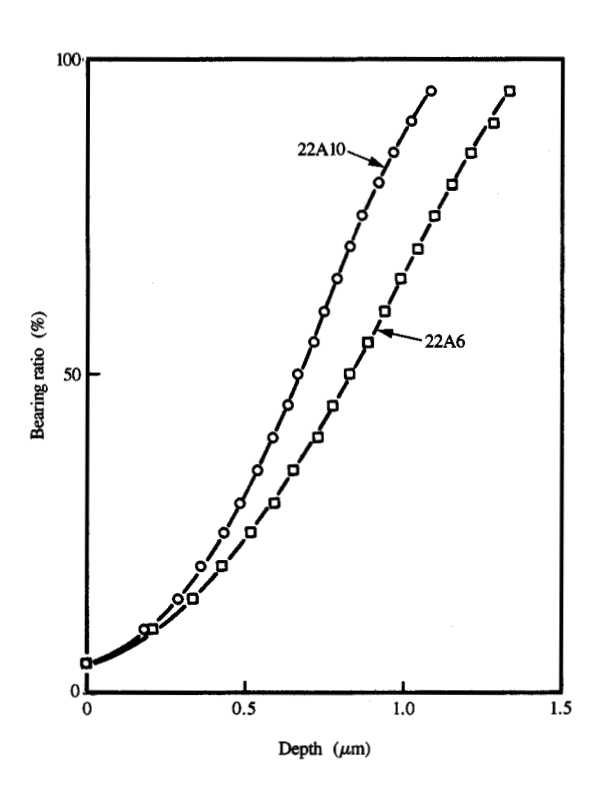
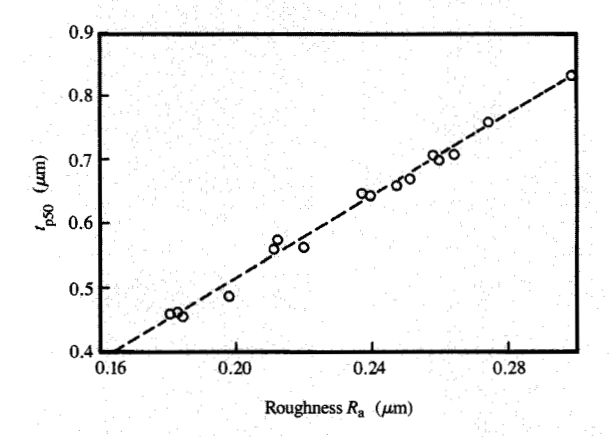


Figure 2

Bearing ratio curves: Bearing ratio as a function of depth for master roll 22A10 ($R_a=0.265~\mu m$, $R_z=1.91~\mu m$) and master roll 22A6 ($R_a=0.342~\mu m$, $R_z=2.38~\mu m$).

stylus and the underlayer. At some "depth," i.e., some distance from a preset baseline, a horizontal "test" line is drawn through the excursions of the profilometer trace; the bearing ratio is defined as the ratio to the measuring length of the sum of those portions of the test line delimited by the excursions of a peak. (The baseline may be fixed at, say, the position giving a 5% bearing ratio.) The bearing ratio, or Abbot-Firestone curve, is a plot of bearing ratio vs. depth. Such a curve for a typical underlayer is shown in Figure 2, from which it may be observed that



Floure 3

 t_{p50} as a function of R_a for calendered master rolls from series 15A.

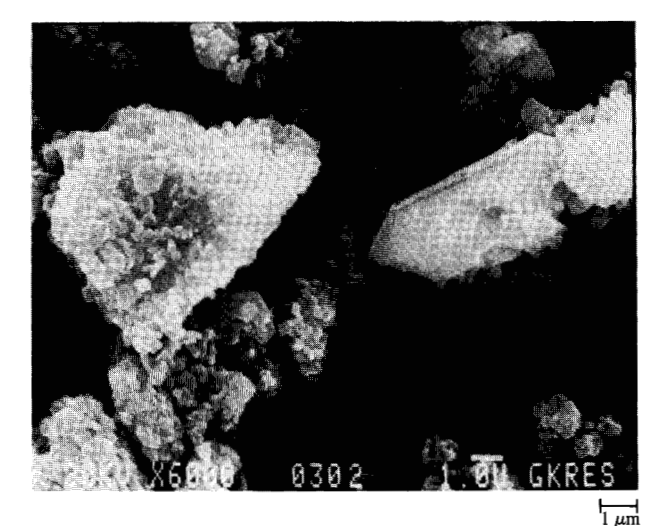


Figure 4

Scanning electron micrograph of silica powder. Courtesy Illinois Mineral Co., Cairo, IL.

meaningful depth variations of the order of 1 μ m are found. A convenient single-parameter description of the bearing-ratio curve may be given by t_{ps0} , which may be defined as the depth corresponding to a 50% bearing ratio.

A direct proportionality was found among R_a , t_{p50} , and R_z , as illustrated in Figure 3 for t_{p50} and R_a for a series of master rolls corresponding to different milling times.⁸

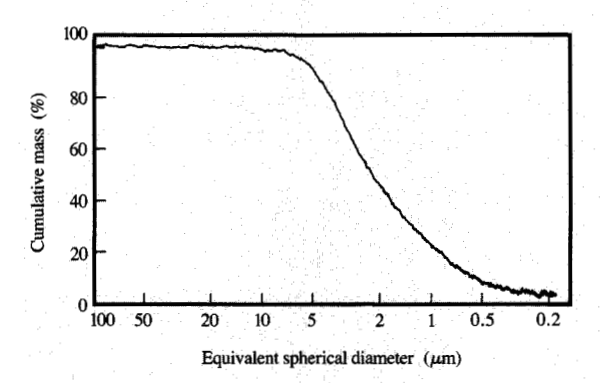


Figure 5

Cumulative particle size distribution for Imsil A108 silica as measured by Coulter counter. Cumulative mass as a function of equivalent spherical diameter.

Despite this proportionality, in practice two of the three parameters were measured to characterize the morphology, usually $R_{\rm a}$ and $R_{\rm z}$, to ensure confidence in the reproducibility of the results. Profilometer traces were usually taken at three positions corresponding to regions across the width of the web at the center, left, and right. Typical values of the standard deviation were 0.01–0.02 μ m for $R_{\rm a}$, and 0.1–0.2 μ m for $R_{\rm a}$.

The present studies have shown that the underlayer morphology as measured by the profilometer was determined primarily by

- The concentration and particle-size distribution of the silica used in the underlayer coating fluid.
- 2. The underlayer thickness.
- 3. The milling conditions employed in the coating-fluid preparation processes.
- 4. The calendering process following the coating procedure.

Influence of silica

As seen from Figure 4, the natural silica used is composed of particles having a wide size distribution. The larger particles are usually conglomerates of many smaller particles. The particle size distribution may be measured by several techniques such as the Coulter counter method [4], with typical results shown in Figure 5. A shift of this distribution in favor of the larger particles, for example, was found to cause a greater surface roughness. Care therefore had to be taken to ensure that the silica used in making the coating fluid had a particle-size distribution which was within specifications in order to maintain the desired surface morphology.

 $[\]overline{8}$ Values of t_{p50}/R_a of about 2.4 to 2.7 were found for master rolls corresponding to widely different values of PVC of the silica. Such values are very close to the value of 2.7 for t_{n50}/R_a obtained from Figure 3.

The concentration of the silica in the coating fluid also had to be controlled carefully, since the roughness was shown to increase monotonically with the PVC⁹ of the silica, as illustrated in **Figure 6**. However, the silica PVC affects not only the surface roughness but also the underlayer hardness. This was shown by microhardness testing of special samples made by spin-coating a 5- μ m-thick film of the underlayer formulation on a silicon wafer; the Knoop hardness was measured with a special microhardness-testing microscope (the "Miniload" hardness tester, Leitz, Germany). The results (**Figure 7**) show that the microhardness increased with increasing PVC but began to saturate at about 20% PVC. Since inadequate underlayer hardness can cause shortened press life (Part III), a PVC of about 20% is desirable.

⁹ As pointed out previously (Part I), the pigment volume concentration (PVC) of a coating is defined as the volume of pigment divided by the total volume of pigment plus binder, where the volume of each component is defined by the ratio of its weight in the formulation to its density.

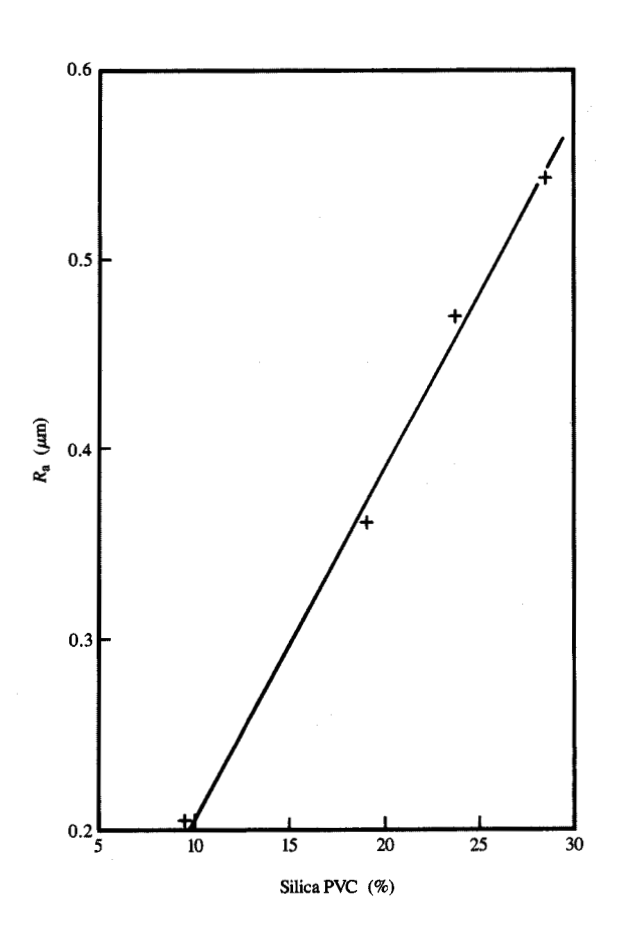


Figure 6

 $R_{\rm a}$ as a function of silica PVC for uncalendered master rolls of series 30A.

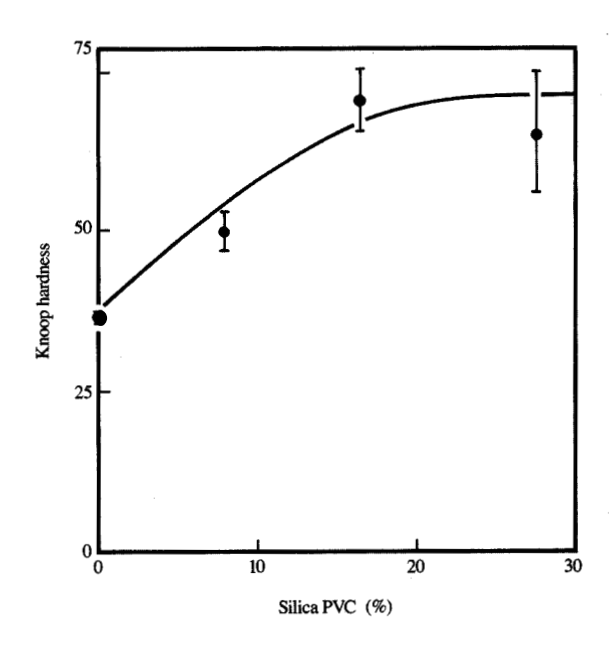


Figure 7

Knoop hardness as a function of silica PVC. Special samples spin-coated on silicon wafers.

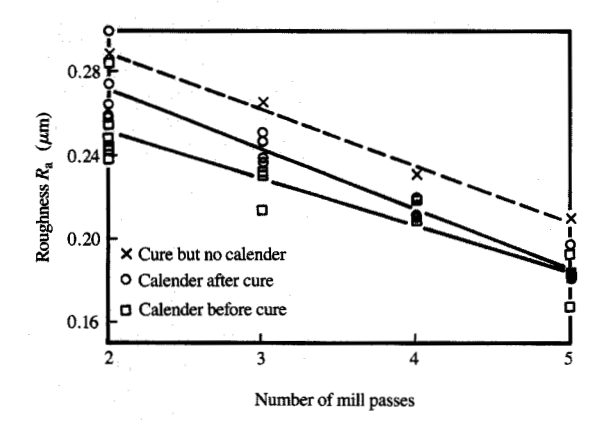
Influence of milling

The silica particles illustrated in Figure 4 are broken down and decrease in size during the milling operations of the coating-fluid preparation procedure; the more vigorous the milling action, the smaller the resulting particle size. It is therefore necessary to maintain strict control of the milling action in order to obtain the specified surface morphology. The grinding action of a media mill is determined by the geometry of the mill, the grinding medium chosen, the concentration and flow rate of the slurry, and the number of passes which the slurry is allowed to make through the mill.

A monotonic decrease in R_a with increasing number of mill passes for a constant flow rate is shown in Figure 8.

Influence of calendering

With good control of the coating-fluid preparation and coating processes, it was usually possible to obtain an initial surface morphology which was reproducible and within a predictable range. However, the subsequent calendering operation caused a decrease in surface roughness, so that this operation also had to be carefully controlled in order to obtain the desired final surface morphology. The effects of the calendering operation can be seen by optical microscopy, as illustrated in Figure 9.



 $R_{\rm a}$ as a function of number of mill passes for master rolls uncalendered but cured, rolls calendered after cure, rolls calendered before cure. Master roll series 15A. Cure conditions: 75°C for 24 h. Calender conditions: 2.28 \times 10⁵ N/m, 93°C.

Table 3 Surface morphology as affected by calendering.

Roll	Mill passes	Before calendering				
		R _a (μm)	$\frac{R_z}{(\mu m)} \frac{R_z/R_a}{R_z}$	R _a (μm)	R _z (μm)	R_z/R_a
28A13A 28A12A 28A6A	3 4 5	0.396 0.330 0.282	3.25 8.21 2.58 7.81 2.17 7.69	0.342 0.283 0.277	2.30 1.90 1.94	6.72 6.71 6.95

- 1. Thickness of underlayer was about 5.0 μm.
- Silica PVC was 17.1%. Formulation A of Table 1 was modified so that saturated polyester concentration was increased to 9-11% of nonpigment solids.
- 3. Cured at 75°C for 24 h.
- Calender conditions: 82°C roll temperature, 3 × 10⁵ N/m linear pressure at 30-60 m/min.

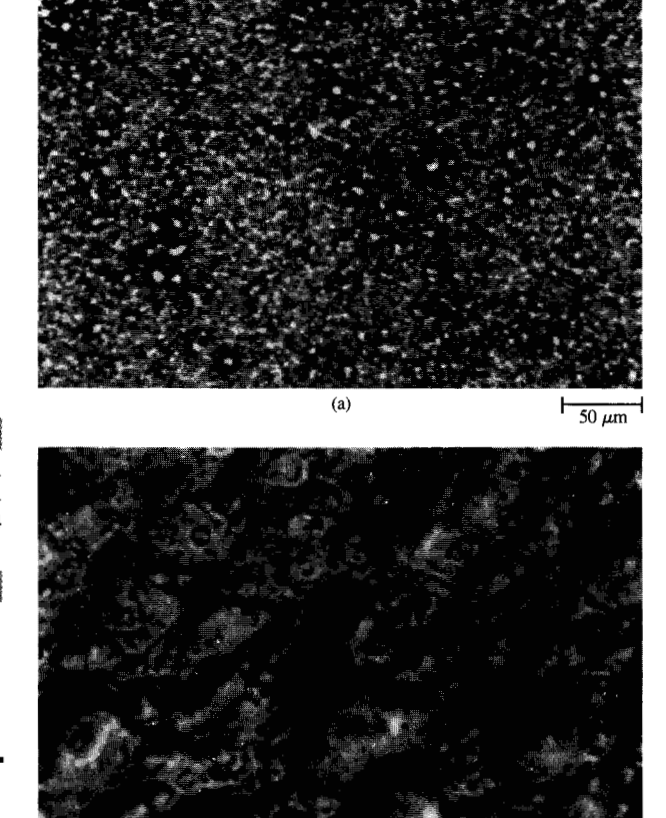


Figure 9

Optical micrograph of master roll after calendering at 6.13×10^5 N/m, $\sim 80^{\circ}$ C: (a) Low magnification. (b) High magnification.

(b)

10 μm

At low magnification, specular reflections from many scattered peaks may be observed [Figure 9(a)]; a high-magnification micrograph reveals that the calendering has smoothed if not flattened these peaks [Figure 9(b)]. The profilometer also shows a decrease in surface roughness caused by calendering; i.e., calendering causes a decrease in the values of R_a and R_a (see Figure 8).

The parameters which control the calendering action are primarily the pressure and temperature in the nip; relatively little effect was seen when the web speed was varied in the range of 25 to 200 m/min. The value of $R_{\rm a}$ decreased monotonically with increasing pressure, as shown in **Figure 10**. The influence of the temperature is

illustrated in Figure 11, which shows a sharp change in slope of the $R_{\rm a}$ curve vs. temperature above a temperature which probably corresponds to the glass transition temperature. In order to maximize the calendering effectiveness, a temperature above 75°C should therefore be used; it was found, however, that temperatures above about 90°C were impractical because underlayer material tended to adhere to the calender rollers.

If both calendering and cure treatments were performed, it was found that the order of these treatments was important. As seen from Figure 8, the decrease in $R_{\rm a}$ caused by calendering was greater when the cure followed rather than preceded the calendering. This result is not

unexpected, because a cure cycle should harden the underlayer and thus make it more resistant to the calendering action.

It is instructive to compare the effect of calendering on R_a and R_z . It is seen from **Table 3** that the decrease of R_z caused by calendering was always substantially greater than that of R_a ; i.e., the ratio R_a/R_a was reduced upon calendering. Since R_{τ} is associated with the largest peaks, this result implies that the calendering action was more effective on the higher peaks, which is consistent with intuition. It may also be noted from Table 3 that the decrease due to calendering of R_{\circ} was more pronounced for rolls associated with fewer mill passes. (The statistical scatter of the data in Figure 8 obscures this conclusion, but the effect has been recorded for many master rolls.) This result is also in accord with intuition, since it would be expected that the calendering effect would be more pronounced for a surface which is initially rougher. It is also interesting to observe that among the various mill passes the *spreads* of both R_a and the ratio R_a/R_a were reduced upon calendering, showing that calendering permitted attainment of a given specification of surface morphology with greater latitude in milling conditions.

It should be noted that calendering typically caused a 5–15% decrease in underlayer thickness. This densification may well be associated with the calendering-induced improvements observed in the cohesion of the underlayer and improvements in the adhesion of the underlayer to the polyester substrate (see Section 5).

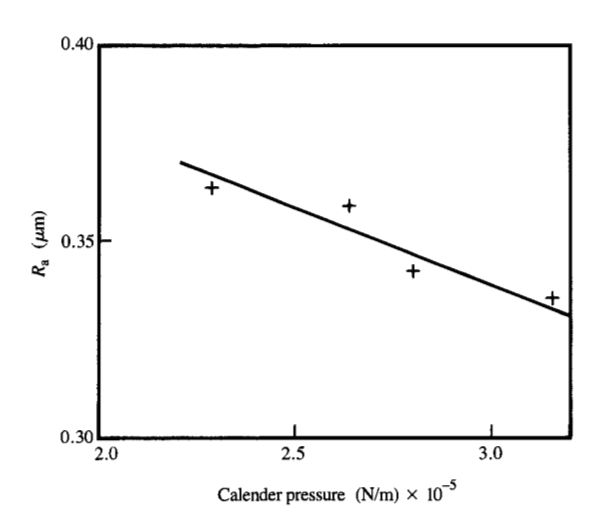


Figure 10

 $R_{\rm a}$ as a function of calender pressure. $R_{\rm a}$ was 0.411 $\mu{\rm m}$ before calendering. Calender temperature was 71.1°C; master rolls were calendered before curing at 100°C for 24 h. Master roll series 194

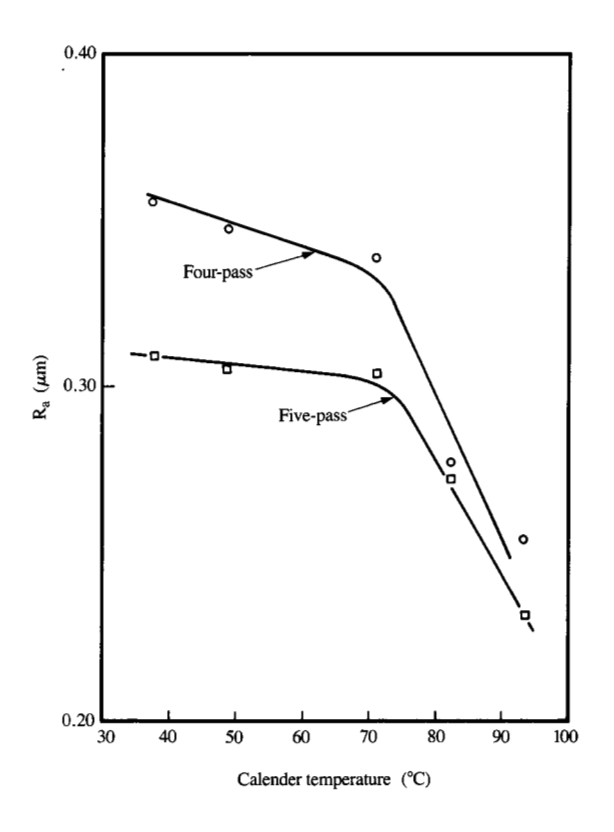


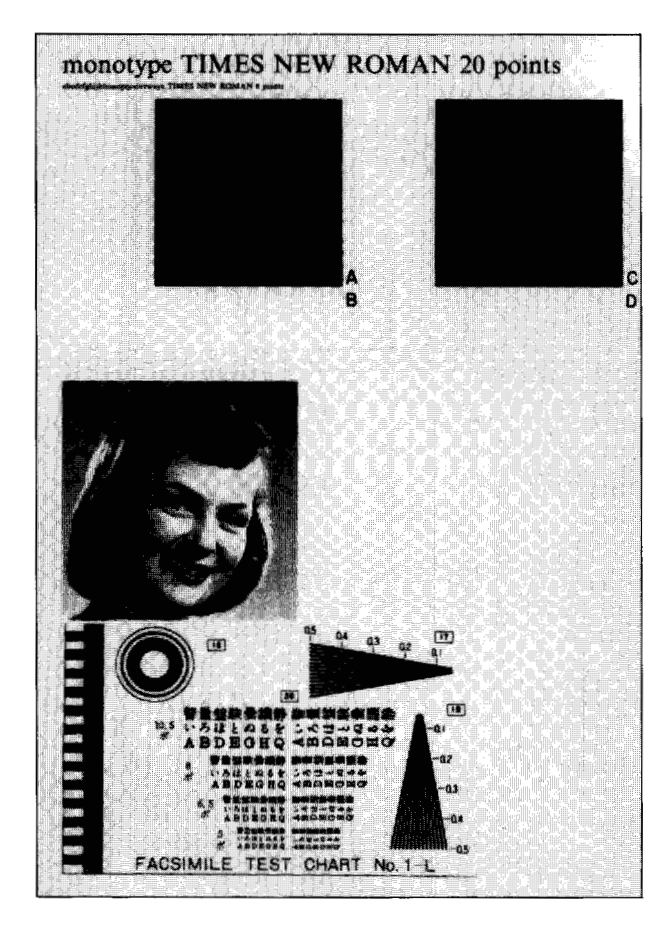
Figure 11

 $R_{\rm a}$ as a function of calender temperature. Before calendering, $R_{\rm a}$ was 0.411 μ m for four-pass rolls and 0.346 μ m for five-pass rolls. Master rolls were calendered before curing at 100°C for 24 h. Master roll series 19A.

Underlayer thickness

The underlayer thickness could be measured in a few representative locations immediately after coating by local removal of the underlayer with a cotton swab moistened with a suitable solvent; an area roughly 1 cm in diameter was practical for this procedure. A sensitive mechanical or electronic micrometer could then be used to compare the thickness of the polyester substrate in the area of removal with that of the substrate plus underlayer in the immediately adjacent region. With this procedure the effect of local variations in polyester thickness could be minimized. After a few trials the coating head could usually be adjusted to give the desired thickness.

A gradual monotonic decrease in $R_{\rm a}$ and $R_{\rm z}$ has been observed for underlayer thickness increased above 5 μ m. However, as illustrated in Table 4, a substantial increase in these parameters was seen for underlayers which were less than 4 μ m thick. This effect may be associated with the fact that for such thin underlayers some of the silica



Test pattern used to check scratching and some writing characteristics. Optical densities were measured by a transmission densitometer at points A, B, C, D. Points A and C are in scratched regions; points B and D represent comparison virgin regions.

 Table 4
 Surface morphology as function of underlayer thickness.

Roll	Thickness	Before calendering			After calendering		
	(μιιι)	$R_{\rm a} (\mu { m m})$	$R_{\rm z} \ (\mu{\rm m})$	$R_{\rm z}/R_{\rm a}$	$R_{\rm a} (\mu {\rm m})$	R_{z} (μm)	$R_{\rm z}/R_{\rm a}$
31A7A 31A6A	3.8 5.0	0.478 0.417	3.59 3.09	7.51 7.41	0.347 0.301	2.24 2.09	6.45 6.94

SiO₂ PVC was 22.0%. Formulation B of Table 10 was used with an increase in silica concentration.

Aged 24 h at room temperature.

particles become comparable in size to the underlayer thickness.

■ Metallization

The two important parameters for metallization, i.e., optical density and electrical sheet resistivity, were

checked in a few representative locations after metallization. For this purpose a standard transmission optical densitometer 10 (in white light) and a four-point electrical probe were used. With some care it was found that the optical density, as measured at five or six equally spaced locations across the web width, usually could be kept constant at about 2 within ± 0.1 optical density units. Reproducibility along the length of the web was also very good.

The electrical sheet resistivity was considered less critical, since the major concern was only that the resistivity not be allowed to become so low that electrical problems would be encountered during the electroerosion writing process. A resistivity above about 1.6 Ω/\square was found to be acceptable.

The problem of defects (voids) in the aluminum film is discussed in Part III.

Overlayer thickness

As discussed above, the fundamental method of controlling the overlayer thickness involved measurements of the flow rate of the overlayer coating fluid to the coating head. If this procedure was carried out carefully, it was usually unnecessary to check the overlayer thickness after completion of the coating process.

Nevertheless, on those occasions which required such a check, the overlayer was selectively removed in local areas by lightly rubbing with a cotton swab dipped in a dilute solution of ammonia. By comparing the optical density in a region so treated with that of the area immediately adjacent, a measurement of the increase in the optical density caused by the presence of the overlayer was obtained. Calibration measurements could be made with relatively thick overlayers for good accuracy; such measurements gave about 0.023 optical density units per $\mu g/cm^2$. A difference in optical density of about 0.07 was thus desired. (This principle of optical-density change has also been used to measure the overlayer thickness during the coating procedure. For this process a dual light source and two detectors were employed, one immediately before and one immediately after the coating head. The outputs of the detectors were fed into a differential logarithmic amplifier to give the optical density difference. A bifurcated fiber-optic bundle was found to be well suited as a dual light source. However, it was found that careful control of the coating-fluid concentration and the flow rate made such monitoring unnecessary.)

4. Problems encountered on the IBM 4250 printer

With the institution of the fabrication procedures and material-property controls discussed above, it became

Calendar conditions: 85°C roll temperature, 5.3 × 10⁵ N/m linear pressure at 60 m/min.

¹⁰ The instrument used was the TD904, Macbeth Div., Kollmorgen Corp., Newburgh, NY.

possible to make DNP material having measurable and reproducible physical properties. The next stage of the development program involved extensive testing of the material on the IBM 4250 printer. These tests revealed the following set of problems, some of which were discussed previously (Part I):

- · Scratching.
- Writing failure.
- Head wear.
- Gouging.
- Fouling.

These failure modes are discussed in detail below together with their corresponding test procedures. ¹¹ Upon analysis of the test results, the fabrication procedures discussed above were modified to minimize these problems.

• Scratch testing

As pointed out in Part I, scratching involves local mechanical removal of aluminum by the moving head even in the absence of firing of the styli (Part I). Scratching was studied by the same technique described in Part I, namely monitoring the associated decrease in optical density.

Standard test patterns were created in order to test scratching and other aspects of writing performance on the IBM 4250 printer. One of the more useful test patterns is shown in **Figure 12**.

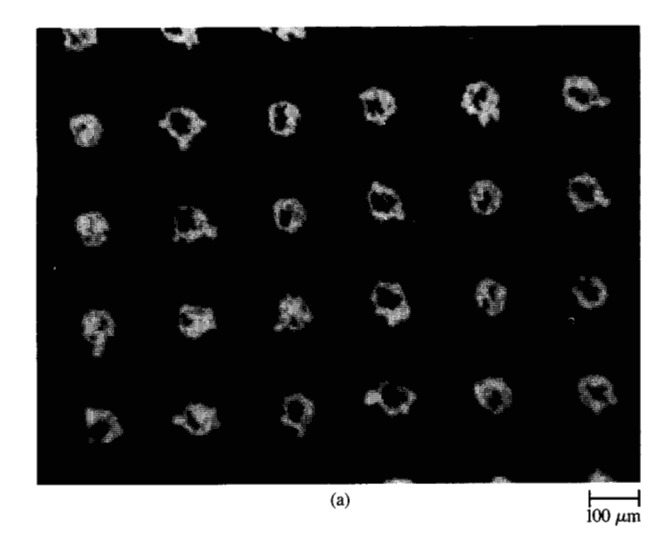
It was found that scratching was most pronounced in those regions immediately following heavily written areas (see Appendix 1). For this reason the scratching associated with the large boxes of the test pattern of Figure 12 was examined as a worst-case check. Specifically, the index of scratching was taken as ΔOD , the difference in optical density as measured with a transmission densitometer between point A in the scratched region and point B in the neighboring virgin (unwritten) area (Figure 12). Here the proximity of points A and B minimizes error originating in any spatial variation of aluminum thickness. As an additional check, measurements were also taken at the pair of points labeled C and D.

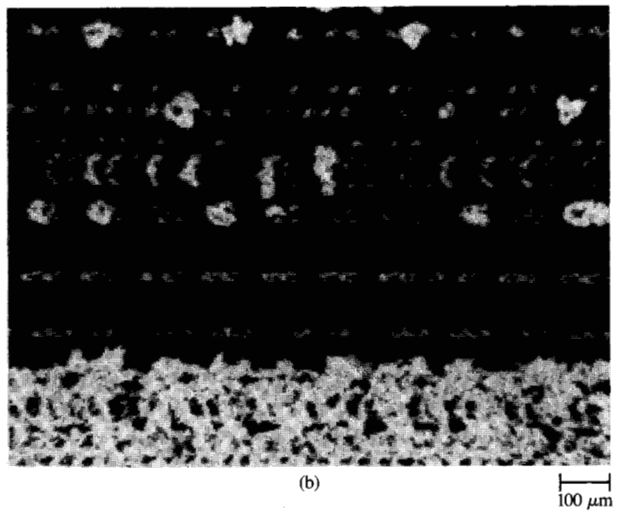
Writing quality

Several semiquantitative tests have been developed which check the adequacy of the electroerosion process for removing aluminum:

Writing failure

The most common manifestation of a writing problem was found to be the appearance of areas in which the electroerosion process failed to remove some or all of the aluminum. This problem was studied with the aid of worst-





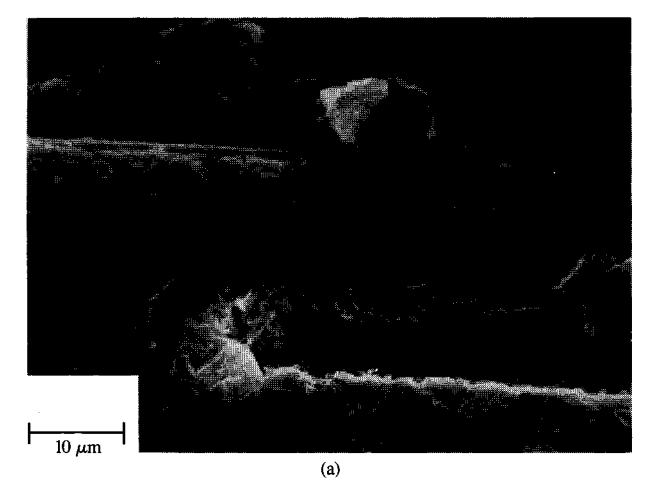
Written areas showing very poor writing characteristics. Master roll 23A2A, written with 2-µs pulse: (a) Square array of pels. (b) Array of fine lines.

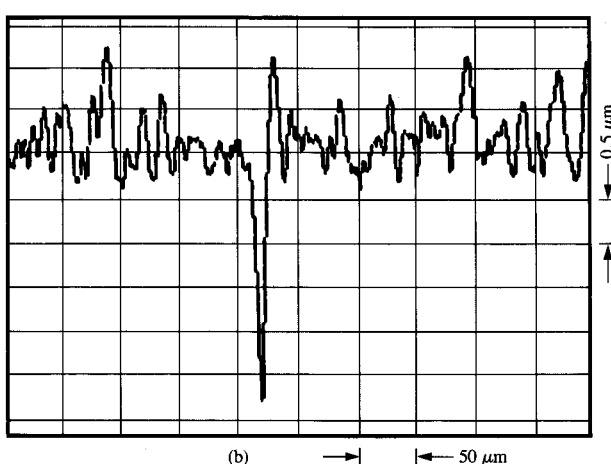
case test patterns involving either a halftone area, i.e., an array of isolated written pels, or an array of fine parallel lines. Writing failure in a halftone region was detected as a reduction in observable image quality caused by a decrease in the correct size of halftone pels, residue left within the written pels, or even their total absence. Writing failure in a fine-line area was represented as a narrowing or even local elimination of the lines. Examples of very poor writing quality are shown in Figure 13 for a roll with too thick an overlayer.

Pel shape and size

The nature of the electroerosion process is such that the periphery of a pel is ragged. Nevertheless, an isolated pel

¹¹ Many contributions to the development of appropriate tests with the IBM 4250 printer were made by J. Bahr and V. Rudolph, IBM Böblingen, Germany.





Gouging: (a) Scanning electron micrograph showing both ends of a typical gouge track with silica particle at one end. (b) Profilometer trace across track showing pronounced depth of gouge.

should approximate a circle with a desired diameter slightly larger than the diameter of a stylus (80 μ m). The size and shape of isolated pels were occasionally checked by optical microscopy.

These studies showed an average pel diameter of about 85 μ m measured perpendicular to the sweep direction, and about 95 μ m in the sweep direction, with a standard deviation of about 8 μ m. The difference in the two diameters may be ascribed to the movement of the head during stylus firing. (These results are typical of rolls with an optical density of about 1.9. A decrease of about 10% in measured pel diameter was observed for an increase in optical density from about 1.8 to 2.1.)

Residual aluminum

Microscopic areas of aluminum were found to remain in an area which had been fully written. These tiny isolated

aluminum islands typically caused an increase in transmission optical density of about 0.1 over that corresponding to an unaluminized sample. Measurements of the transmission optical density within the large boxes of Figure 12 thus provided a warning of excessive residual aluminum.

Head wear and gouging

Both head wear and gouging may be observed with similar test procedures and also appear to be caused by related phenomena.

Basic studies

The fundamental characteristics of head wear and gouging were not explored in the initial study (Part I) because they are associated only with large areas of DNP material.

Stylus wear occurs despite the fact that the writing styli of the IBM 4250 electroerosion head are constructed of a hard metal (tungsten). The writing head contains reserve tungsten wire, so that at intervals fresh wire is fed to the head to compensate for this wear whenever a special sensor detects inadequate styli lengths. The rate of wear of the styli is nevertheless a concern, because excessive wear could prematurely deplete the reserve of tungsten wire and thus shorten the life of the head. High wear of the styli has been observed for DNP material of very high roughness, and particularly for DNP material with inadequate cohesion of the silica particles to the underlayer. The relative motion of the styli with respect to loosened silica apparently causes accelerated tungsten wear.

Another problem is the occasional appearance of "gouges." A gouge represents a "trench" dug through the aluminum layer and deep into the underlayer beneath during the passage of the head (Figure 14). (Gouging should thus not be confused with scratching, for which no underlayer but only aluminum is removed for good DNP material.) Gouges of many different widths have been seen, but their widths are always less than the 80-µm stylus diameter (typically 10 μ m for the widest gouges). Gouges can vary in length from less than 1 mm to many cm. Gouging is a serious problem because the wide gouges can reproduce as an undesired mark either in the directnegative or direct-plate mode. Gouging was not encountered in the previous study of small samples of DNP material (Part I) simply because it is a relatively rare phenomenon; even for poor-quality DNP material which has been written over its full surface, the gouge concentration should be only tens of gouges per square meter.

Both micrographs and profilometer traces showed that the depth of a gouge was essentially the full thickness of the underlayer (Figure 14). This was further confirmed by experiments in which portions of the underlayer immediately surrounding a gouge were stripped off with

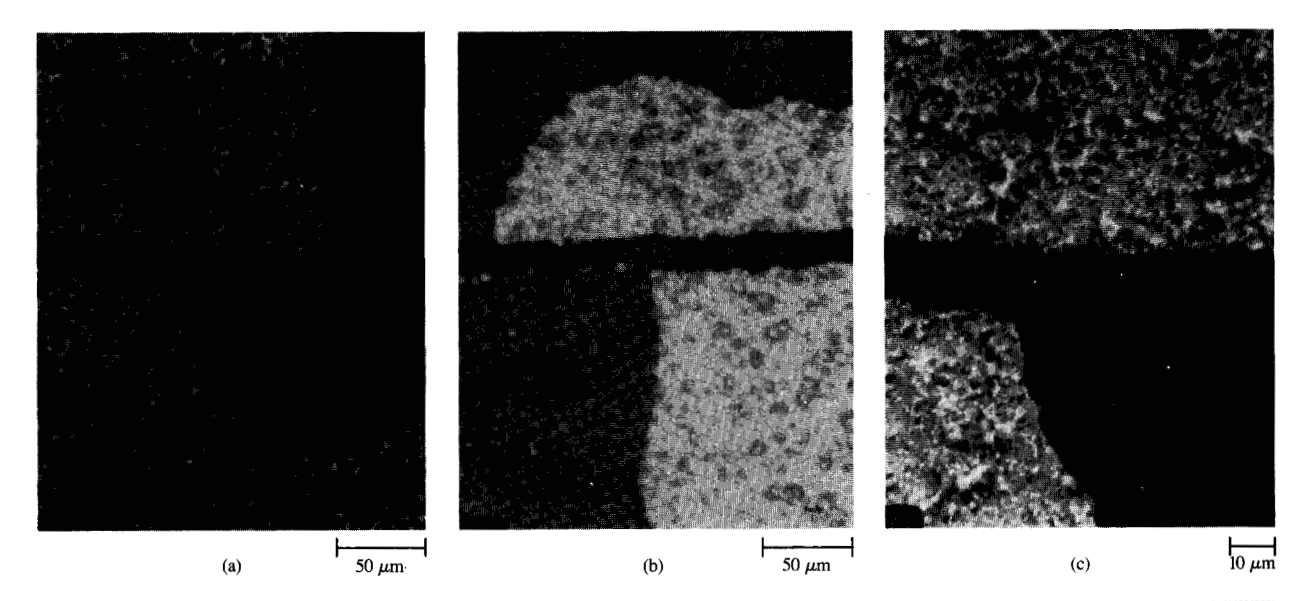


Figure 15

Pressure-sensitive-tape stripping of underlayer from polyester substrate at a gouge: (a) Micrograph of gouge area in DNP material after stripping. Dark area represents stripped-away region; mottled area represents unstripped region. (b) Micrograph of tape surface after stripping. White area represents stripped-away underlayer; darker area represents bare tape surface. (c) High-magnification micrograph of gouge area in DNP material after stripping. In gouge track itself there is neither unstripped underlayer in (a) nor stripped-away underlayer in (b); note striations in gouge track in (c), indicating penetration through underlayer and into polyester substrate.

pressure-sensitive tape (Figure 15). Most of the underlayer in the gouge area came off on the tape except in the region corresponding to the gouge itself; that area remained clear on the original surface [Figure 15(a)] as well as on the tape [Figure 15(b)], showing that no material remained at the bottom of the gouge after the gouging action. Also, striations cut into the polyester substrate within the boundaries of the gouge were visible [Figure 15(c)], again showing that material-removal action during the gouge process occurred all the way down to the polyester substrate.

It is thought that a gouge is formed by a two-step mechanism: First one or more silica particles are dislodged from the underlayer by a moving stylus, and move with it. Second, the moving silica particles act as a knife by completely removing underlayer material in those regions where the adhesion of the underlayer to the polyester substrate is inadequate. Gouging is thus postulated to be associated with inadequate *cohesion* of the silica to the underlayer matrix, along with inadequate *adhesion* of the underlayer to the polyester substrate.

Support for this interpretation may be found in several facts:

 If gouges were initiated by the stylus itself, the gouge width would be comparable to the width of the stylus.
 A considerably smaller gouge width is in fact always

- observed (Figure 14). Silica particles are actually often found deposited at the end of a gouge [Figure 14(a)]; such particles may have been active in creating the gouge.
- 2. Gouges extend in depth down to the polyester substrate, as shown in Figures 14 and 15. Also, strip-off of the underlayer with pressure-sensitive tape occurred only in the areas immediately adjacent to gouges, showing localized weakened underlayer-substrate adhesion in gouge-prone regions. In addition, thinner underlayers were found to exhibit much larger gouge concentrations than did thicker underlayers, presumably because of better propagation of shear stresses to the underlayer-substrate interface in the former case.
- Measures designed to improve the cohesion and adhesion of the underlayer were found to decrease the gouge concentration (see the following).

Measurement techniques

Both head wear and gouging were observed during the sweeping motion of the head across the web, during 100% writing (the styli firing at every pel position), during 0% writing (no firing of the styli), and with intermediate states of writing. A strong dependence of gouge concentration on percentage of writing has not been observed, but lower head wear has been seen with 100% writing compared to 0% writing (see Appendix 1). For this reason both of these

Roll	R _a (µm)	$R_{z} (\mu m)$	Calen- dered?	Al OD	Overlayer thickness (µg/cm²)	ΔΟD
20A7A	0.339	2.61	No	1.81	3	0.21
20A7C	0.311	2.24	Yes	1.84	3	0.09
19A4A	0.311		Yes	1.91	2	0.22
19A4B	0.311		Yes	1.87	3	0.15
19A4C	0.311		Yes	1.89	4	0.09
19A4D	0.311		Yes	1.96	6	0.07
30A8	0.327	2.22	Yes	2.18	3	0.22
29A3B	0.352	2.29	Yes	1.88	3	0.09

For master rolls corresponding to all entries except the last, silica PVC was i7.1%, and Formulation A of Table I was used. For master roll corresponding to the last entry, the silica PVC was 17.3% and Formulation B of Table 10 was used.

phenomena could be examined simultaneously in a worst-case test involving the institution of repetitive nonfired sweeps of the head. The test was continued for about 4000 sweeps, which is equivalent to about 5 linear m or 1.3 m² for a sweep length of about 25 cm.

Insufficient stylus length due to head wear is automatically sensed by the IBM 4250 printer, causing compensating advances of the styli in 4- μ m increments. The average number of head sweeps between automatic styli advances was thus available as a convenient index of head wear, which could be expressed as the number of sweeps per micron of styli advance. (A high value of the head wear index thus indicates a *low* wear rate.)

The gouges were counted and qualitatively classified as very narrow, narrow, and wide, where wide represented gouges approximately $10~\mu m$ in width. Only those gouges in the latter category were included in the final statistics, because only they were found to reproduce during printing either from a direct negative or direct plate. Although gouge lengths varied widely from submillimeter to several centimeters long, the results were expressed as the number of wide gouges per square meter; gouge concentrations quoted in the present paper are to be interpreted in this manner.

Fouling

As pointed out in Part I, the production of debris is inherent in the electroerosion process. If the underlayer and overlayer were formulated correctly, this debris was found to consist of light, free-flowing particles, so that the effects on the writing action were minimized. Some of this debris was found to deposit on the insulator block between the protruding styli, filling that space up to the level of the styli tips after a few sweeps. This debris normally did no harm in the *short term* because it was scoured off the styli by the motion of the head across the rough DNP material.

However, that portion of the debris on the writing head which was immediately adjacent to the insulating block was found to transform slowly into a very hard cake which grew in thickness with continued writing, and which could be removed only by vigorous scraping with a hard tool. Eventually the buildup of this hard cake proceeded to a point where the cake grew up to the level of the styli tips, at which time the writing quality deteriorated badly, thus presenting a potential *long-term* fouling problem. While the cycle of debris production, distribution, and transformation is poorly understood, measurement techniques have nonetheless been developed to monitor the buildup of the hard cake and its effect on writing.

In such tests the IBM 4250 printer was adjusted for continuous 100% writing. During a test the head was periodically removed and given a light mechanical brushing with a soft-bristle brush; this treatment was adequate to remove the overlying powdery debris layer. The average height of the remaining hard cake was then determined with a low-powered microscope. In this way the buildup of the hard cake was monitored as a function of the number of writing sweeps; this information was then used as an indication of fouling of the head. The data were most conveniently expressed as the percentage buildup of the hard cake, where 100% buildup means that the cake extends from the insulating block to the tips of the styli, so that writing efficiency is seriously impaired.

In an alternative test the IBM 4250 printer was kept running continuously until fouling of the head began and consequent signs of poor writing were noticed. For good DNP material, deterioration of writing quality due to fouling requires many hundreds of thousands of sweeps, which represents an acceptable lifetime for the head.

5. Optimization studies

After the achievement of good control of materials characteristics through control of the fabrication processes, and after the institution of appropriate testing procedures, efforts were instituted to optimize the structure of the DNP material. Materials optimization was needed to minimize the problems of scratching, writing failure, head wear, gouging, and fouling, as defined previously. In most cases several factors affected each of these failure modes, so that carefully controlled experiments were required. A further complication arose from the fact that changes in the DNP material structure which produced improvement with respect to one problem often caused worsening of another problem, thereby necessitating compromises in the optimization process.

• Optimization for scratching

As was pointed out previously (Part I), scratching may be reduced by 1) decreasing the surface roughness, and 2) increasing the thickness of the lubricating overlayer. These

^{2.} Various cure and calendering conditions were used for these master rolls.

Table 6 Writing quality in various DNP materials.

Roll	R _a (μm)	R _z (μm)	Mill passes	Pulse length (µs)	Overlayer thickness (µg/cm²)	Halftone quality	Fine-line quality	Box OD
23A2A	0.268	2.31	6	3	3	VB	VB	0.11
23A5A	0.322	2.66	4	3	3	OK	OK	0.13
23A5A	0.322	2.66	4	3	3	OK	OK	0.13
20A10	0.333	2.30	7	3	5	P	P	0.12
20A10	0.333	2.30	7	1	5	VB	VB	0.16
20A10	0.333	2.30	7	2	5	В	В	0.12
20A10	0.333	2.30	7	3	5	P	P	0.12
20A10	0.333	2.30	7	5	5	OK	OK	0.11
20A10	0.333	2.30	7	7	5	OK	OK	0.10
20A10	0.333	2.30	7	15	5	В	В	0.09

- 1. VB = very bad; B = bad; P = poor (some defects); OK = acceptable (no defects).
- 2. Silica PVC was 17.1%. Formulation A of Table 1 was used.
- 3. Cured at 24 h at 90–105°C
- 4. Calender conditions varied among master rolls
- 5. All master rolls had aluminum with approximately 1.9 OD.

relationships were found to hold in the present study as

Upon comparing the first set of entries in **Table 5**, it is seen that a decrease of more than a factor of 2 is obtained in ΔOD when the roughness is decreased by calendering action. Similar effects have been seen for changes in roughness caused not by calendering but by changes in milling time of the underlayer coating fluid, by changes in the PVC of the silica in the underlayer, or by changes in the underlayer thickness (Section 3). The next set of entries of Table 5 illustrates the decrease in scratching associated with increasing thickness of the overlayer.

The third set of entries of Table 5 shows a marked decrease in ΔOD when the thickness (the OD) of the (unscratched) aluminum is decreased. However, if all other factors are held constant, the areal fraction of aluminum removed during scratching is independent of aluminum thickness, as pointed out in Appendix 2, so that the index ΔOD is somewhat misleading in this case. The aluminum thickness is thus not a major factor in optimization for scratching.

• Optimization for writing

The writing quality was found to depend on the roughness of the underlayer, the thickness of the overlayer, the pulse length, and the thickness of the aluminum.

The first set of entries in **Table 6** illustrates the dependence of writing quality on underlayer roughness. It is seen that some writing difficulties are encountered when the underlayer roughness is too low. As was pointed out (Part I), this problem may originate in the fact that an underlayer which is too smooth leads to a very low-resistivity stylus—aluminum contact. For such a contact the portion of the writing pulse devoted to phase 1 becomes so large that little time is left for phase 2, which is responsible

for the removal of most of the aluminum. Another factor may well be the inadequate scouring action of a low-roughness underlayer for which debris can build up at the tip of the styli, thereby affecting the local aluminum-stylus conductivity (Part I).

The second set of entries in Table 6 illustrates the influence of the overlayer thickness on writing quality. An increase from 3 to 5 μ g/cm² causes a marked deterioration in writing quality because of the additional material to be removed in the electroerosion process.

The third set of entries in Table 6 shows that the initially poor writing quality improved as the pulse length increased. (The poor writing quality at low pulse lengths shown in the third set of entries of Table 6 probably was caused by the relatively large thickness of the overlayer.) The increased pulse length presumably permitted completion of the prolonged phase 1 portion of the pulse for this sample. However, for very long pulse lengths a degradation in writing quality was observed, probably because under those circumstances the styli became very hot so that debris adhered to them (see Appendix 1). The last column of Table 6 shows the optical density of the fully written boxes of the test pattern shown in Figure 12. This optical density is a measure of the presence of residual aluminum after writing; as expected, there was less residual aluminum when the writing pulse length increased.

Other tests indicated, as anticipated, that as the aluminum thickness increased the writing quality decreased, as judged by the deterioration in the quality of halftones and arrays of fine parallel lines.

Optimization for head wear and gouging The related subjects of head wear and gouging may be discussed together because, as pointed out earlier,

Number of wide gouges/m² as a function of the concentration of saturated polyester in underlayer for Formulation B (Table 8).

Concentration saturated polyester (%)

Table 7 Head wear in various DNP materials.

Roll	Calen- dered?	R _a (μm)	Mill passes	Head wear index (Sweeps/μm)
9A11-1	No	0.389	1	12
9A11-2	No	0.371	2	16
9A11-3	No	0.333	3	18
9A11-4	No	0.328	4	54
11A1	No		4	24
11A1	Yes	0.225	4	165
11A2	No		4	26
11A2	Yes	0.209	4	205

Silica PVC was 17.3%. Formulation A of Table 1 was used.

measures which decreased head wear were usually observed to decrease gouge concentration simultaneously. It is shown in this section that gouging and excessive head wear can be suppressed by use of various techniques which 1) remove large silica agglomerates, 2) improve the cohesion of the underlayer, and 3) improve the adhesion of the underlayer to the substrate. Such techniques include good milling, dispersing, and filtering of the underlayer coating fluid, and calendering and curing of the coated web. A modification of the coating-fluid formulation was also shown to offer some benefit, as was an increase in underlayer thickness.

If no calendering treatment was given, it was found that head wear decreased as the surface was made smoother. This is shown by the first set of entries of Table 7, where a correlation is seen between increasing head wear index and decreasing R_{\perp} caused by increasing the number of mill passes during the underlayer coating-fluid preparation. A calendering treatment was also found to cause a pronounced decrease in head wear, as illustrated by the second set of entries in Table 7.

Similar trends have been observed for the gouge concentration; i.e., avoidance of excessive roughness along with the use of calendering yielded lower gouge concentrations. For the greatest gouge reduction the calendering action should be as effective as possible, i.e., be carried out at high temperatures and pressures for long durations. In one case, for example, it was found that a master roll which had been calendered at 2.1×10^5 N/m at 99°C had 14.7 gouges/m², while an identical roll calendered at 3.0×10^5 N/m at 99°C had 6.4 gouges/m². For this reason vigorous calendering was routinely used in the fabrication of most of the master rolls.

One of the reasons for the effectiveness of the calendering treatment may be that it decreases the concentration of loosely held silica particles which are associated with widely scattered very high peaks comprising large agglomerates of silica particles. 12 The calendering action on such high peaks is probably to crush them into the underlayer (see Figure 9), which is in plastic flow at the calendering temperatures and pressures. The densifying action of the calendering treatment in fact probably leads to a general improvement of the cohesion of the underlayer.

As was pointed out above, while pickup of silica particles by the stylus may initiate a gouge, the gouge is subsequently propagated by the rupture of the underlayer-substrate bond. It is therefore important to ensure good underlayer-substrate adhesion. The choice of a polyester substrate which incorporates a thin adhesionpromotion primer has been shown to be helpful in this

Cured either at room temperature or 60°C for 24 h. Calender conditions (for calendered master rolls): 90°C master roll temperature, 3.5×10^5 N/m linear pressure at 90 m/min.

¹² There is also some evidence that use of a 20-μm filter instead of a 40-μm filter at the coating head leads to decreased gouge concentration, again because of removal of silica agglomerates. This result was obtained by T. J. Marsh of IBM Boulder.

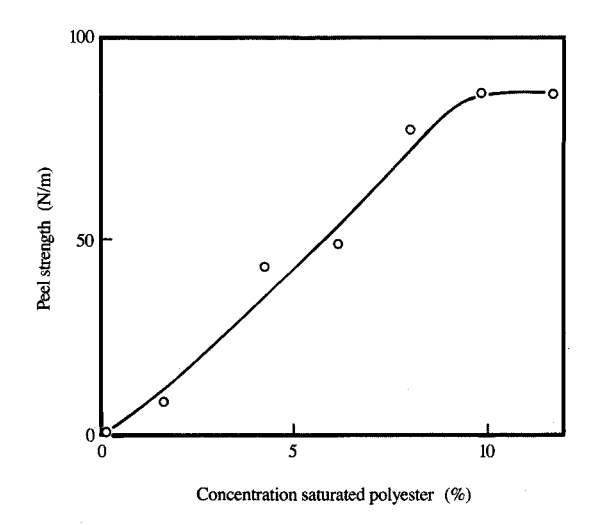
regard. Tests indicate that this prime layer should be continuous and of adequate thickness, and should have a relatively low cross-linking density within it.

An improvement in underlayer-substrate adhesion was also achieved by a modification in the coating-fluid formulation. This modification (Formulation B, Table 8) involved primarily a simple increase in the concentration of the saturated polyester dispersant 13 from the values given for Formulation A in Table 1. As the concentration of this polyester dispersant was increased, the gouge concentration decreased monotonically (Figure 16). This effect may be related to improved underlayer-substrate adhesion with increasing polyester-dispersant content, as shown by quantitative strip-off tests 14 (Figure 17). The improved adhesion may be related in turn to an improvement in the reaction between the polyester primer coat and the underlayer caused by the fact that increased saturated polyester content lowers the glass-transition temperature of the underlayer; i.e., it acts as a plasticizer. Because of this plasticizing action, calendering may also be rendered more effective in improving the cohesion of the underlayer.

A practical result was achieved when the concentration of the saturated polyester was increased to 11.8% of the total nonpigment solids for Formulation B, compared to 1.7% for Formulation A.

The cure treatment was found to be another important factor. As shown in Table 9, cure treatments of a given roll at successively increased temperatures caused marked decreases in the gouge concentration. The head wear simultaneously decreased, again illustrating the connection between gouging and head wear. It is thought that the cure treatment was effective in both cases because it simultaneously improved the cohesion of the silica within the underlayer and the adhesion of the underlayer to the substrate.

Many master rolls were made with a cure treatment of 90-100°C for about 24 h, followed by a calendering treatment. Such rolls exhibited low gouge densities (about 1 gouge/m² or less). As pointed out previously, however, it was found that such high-temperature cure treatments caused unacceptable distortion of the polyester substrate. If the cure temperature was decreased to about 50-75°C, gouge suppression was less effective, but little substrate distortion was found.



Adhesion of underlayer to polyester substrate (peel strength) as a function of concentration of saturated polyester in underlayer for Formulation B (Table 8).

Table 8 Coating liquid for underlayer: Formulation B.

Component	Description	Parts by weight
Mill base		
17% CAB solution		20.00
Silica (particles):	Imsil A108	20.10
Saturated polyester:	Multron R221-75	6.80
Polytetrafluoroethylene	du Pont Teflon® DLX-	
(particles):	6000	0.94
Surfactant:	Gafac RE-610	0.10
Let-down Mill base listed above Isocyanate cross-linker: Solvent: Solvent: Catalyst:	17% CAB solution Mondur CB-75 Methyl ethyl ketone Toluene Dimethylamino ethanol	94.30 24.70 36.75 4.08 0.04
Flow agent:	FC-430	0.12
17% CAB solution Solvent: Cellulose acetate butyrate: Solvent:	Methyl ethyl ketone Eastman CAB 553-0.4 Toluene	74.7 17.0 8.3

PVC SiO₂ = 17.3%; PVC polytetrafluoroethylene = 0.93%. Saturated polyester is 11.8% of nonpigment solids, or 26.25% of CAB.

M. S. COHEN ET AL.

¹³ In addition to the increase in saturated polyester dispersant, a surfactant was added to Formulation B to improve the dispersal of the silica particles, which served to improve their cohesion to the binder. In addition, a catalyst was added to increase the cross-linking reaction rate. It may also be noted that CAB solution was added to the let-down in Formulation B. This step permitted efficient milling with a high concentration of silica particles, with subsequent reduction of the silica PVC

by the CAB addition during let-down.

14 In these tests a narrow polyester ribbon was cemented to the underlayer with epoxy resin; the polyester substrate was in turn cemented to a metal block. The sample was put into an instrument which applied a measured vertical force to the end of the ribbon; this force was gradually increased until the underlayer was pulled from the polyester substrate (Instron Engineering Corp., Canton, MA)

CAB 553.4, Eastman Chemical Products, Kingsport, TN.

Imsil A108, Illinois Mineral Corp., Cairo, IL. Multron R221-75, Mobay Chemical Corp., Pittsburgh, PA

Teflon DLX-6000, E. I. du Pont de Nemours & Co., Wilmington, DE.

Gafac RE-610, GAF Corp., New York, NY. Mondur CB75, Mobay Chemical Corp., Pittsburgh, PA.

FC-430, 3M Corp., St. Paul, MN

Table 9 Effect of curing on gouging and head wear.

Roll	Calendered?	$R_{ m a} \ (\mu{ m m})$	$R_{z} \ (\mu \mathrm{m})$	Cure temp. (°C)	Gouge concentration (No./m²)	Head wear index (Sweeps/μm)
20A6B	Yes	0.319	2.13	90°C for 48 h	11.0	265
20A6B	Yes	0.319	2.13	110°C for 16 h	1.3	320
20A6B	Yes	0.319	2.13	122°C for 15 h	0.6	438

The same master roll was given three successive cure treatments.

Table 10 Effect of underlayer thickness on gouging.

Roll	Underlayer thickness (μm)	$R_{ m a} \ (\mu{ m m})$	R _z (μm)	Gouge concen- tration (No./m²)
31A7A	3.81	0.347	2.24	64
33A3A	4.83	0.302	2.13	11.0
33A3B	5.36	0.338	2.06	0.8
33A3C	6.20	0.285	1.98	0

Silica PVC was 22.0%

The results described thus far were obtained primarily with DNP material having an underlayer thickness of about 5 μ m. It was found, however, that an increase in underlayer thickness to about 6 µm gave a pronounced decrease in gouge concentration without adversely affecting other properties 15 (Table 10). The gouge concentration is greater for thin rather than thick underlayers because, as pointed out earlier, in thin underlayers shear stress is more easily transmitted to the underlayer-polyester interface. Also, a very thin underlayer may not permit the calender-induced crushing of the high peaks. An increase in underlayer thickness was so effective in reducing the gouge concentration that for material having a thick (about 6 μ m) underlayer, the hightemperature cure could be replaced by a 24-h aging at room temperature. Such material still exhibited gouge concentrations less than 1/m² for either formulations A or B.

• Optimization for fouling suppression

As noted above, the fundamental mechanisms involved in fouling are poorly understood. Nevertheless, fouling testing carried out on the IBM 4250 printer revealed several facts (Table 11):

- 1. Hard-cake buildup originates in the arcing process. This is illustrated by the first set of entries of Table 11, which shows hard-cake buildup for 100% writing but not for 0% writing.
- 2. Although some of the debris incorporated into the hard cake originates in the aluminum film and in the underlayer, the largest proportion comes from the overlayer. This is illustrated in the second set of entries of Table 11.
- 3. The shorter the pulse length, the less the hard-cake buildup, as shown by the third set of entries of Table 11.

It is not surprising that the overlayer should be a major contributor to the fouling process, since it lies between the styli and the aluminum and is thus subjected to the intense heat of the arc during the electroerosion process. For this reason the overlayer should be as thin as possible consistent with good lubrication. Furthermore, a low binder concentration should be used in the overlayer, and the binder chosen should have as high a glass-transition temperature as possible. (For similar reasons the fluorocarbon which is incorporated in the underlayer may also help to suppress fouling. Some fluorocarbon particles may be picked up by the moving styli, and because of their relatively high glass-transition temperature the debris composite may be rendered less gummy and hence less prone to hard-cake buildup.)

It is known that for very long pulses the arc can extend well beyond the edge of the tungsten stylus (Part I). It is postulated that under these circumstances the overlayer in such peripheral regions can reach unusually high temperatures because the stylus is not close enough to conduct away excess heat. At such high temperatures the debris becomes soft and gummy so that it is more easily picked up and compacted into the hard cake, thus accelerating fouling (see Appendix 1). By reduction of the pulse length to the minimum value yielding acceptable pel sizes (about 80 to 90 μ m), this effect is minimized. ¹⁶ In the earlier experiments a pulse length of 3 μ s was used. A pulse 1 μ s long gave a very substantial reduction in fouling

PVC of SiO₂ was 17.1%. Formulation A of Table 1 was used. Cured at 90°C for 24 h.

Calender conditions: 100°C master roll temperature, 2.5 × 10⁵ N/m linear pressure at 30 m/min.

Formulation B of Table 8 was used with an increase in silica concentration.

Cured at room temperature for 24 h.

^{4.} Calendar conditions: 85°C master roll temperature, 5.3 × 10⁵ N/m linear ressure at 60 m/min.

^{5.} Underlayer thicknesses given are after calendering; thicknesses before calendering were 10-15% higher.

¹⁵ The data of Table 10 represent results for material made with Formulation B. Similar results were obtained with Formulation A.

¹⁶ V. Rudolph of IBM Böblingen, Germany, contributed to this important insight.

Table 11 Fouling studies.

Roll	R _a (μm)	R _z (μm)	Overlayer thickness (µg/cm²)	Writing (%)	Pulse length (µs)	No. sweeps (× 10 ⁻³)	Hard-cake buildup (%)
18A6	0.287	1.85	3.0	100	3.0	12	22.0
18A6	0.287	1.85	3.0	0	3.0	15	0
19A3	0.310	2.20	0	100	3.0	70	0
19A3	0.310	2.20	3.0	100	3.0	70	17.7
R4-2	0.270	_	3.0	100	3.0	385	11.0
R4-2	0.270	_	3.0	100	1.0	300	2.0

- 1. PVC of SiO2 was 17.1%. Formulation A of Table 1 was used.
- Master rolls corresponding to first four entries were cured at 100°C for 24 h. Master rolls corresponding to last two entries were given different cure treatments, but results were similar.
- Master rolls corresponding to first four entries had calender conditions as follows: 70-90°C roll temperature, 2-7 × 10⁵ N/m linear pressure at 60 m/min. Master rolls corresponding to last two entries were calendered differently, but results were similar.

but too small an eroded pel diameter; 2 μ s was therefore chosen as a good compromise. Under these circumstances only about 5% hard-cake buildup was observed after 100% writing about 150 m² of DNP material.

- General optimization decisions
 Optimization of the individual parameters led to contradictory requirements:
- 1. A rougher underlayer surface (higher values of R_a and R_z) contributes to improved writing quality. However, if the surface is too rough, the scratching, head wear, and gouging can become pronounced, and the written pel shape can become too irregular.
- 2. A thicker overlayer contributes to reduced scratching. However, if the overlayer is too thick, the writing quality suffers and the fouling may become unacceptable.
- 3. Thinner aluminum contributes to improved writing.

 However, if the aluminum is too thin, excessive light may be transmitted through it in the unwritten (background) areas during use as a direct negative (see Part III)
- 4. A vigorous calendering operation (high temperature and pressure) along with a thick underlayer contributes to reduced head wear and gouge concentration. However, if either the calendering treatment is too severe or the underlayer is made too thick, the underlayer surface can become so smooth that the writing quality suffers.
- 5. A longer pulse length can give improved writing but can lead to increased head fouling.
- A higher cure temperature can reduce the gouge concentration but can cause distortion of the polyester substrate.

It is fortunate that compromise choices can be made to give a processing "window" which yields acceptable DNP material:

- 1. Before calendering the roughness should be 0.37 μ m $< R_a < 0.42 \ \mu$ m, with 3.0 μ m $< R_z < 3.5 \ \mu$ m. After calendering the roughness should be 0.29 μ m $< R_a$ $< 0.34 \ \mu$ m, with 1.8 μ m $< R_z < 2.3 \ \mu$ m. ¹⁷
- 2. The overlayer thickness should be between 3 and $4 \mu g/cm^2$.
- 3. The aluminum thickness should be such that the transmission optical density is between 1.8 and 2.0.
- 4. The underlayer thickness after calendering should be about 6 μm .
- 5. A writing pulse length of 2 μ s should be used.
- 6. A cure treatment as mild as a 24-h aging at room temperature may be used.

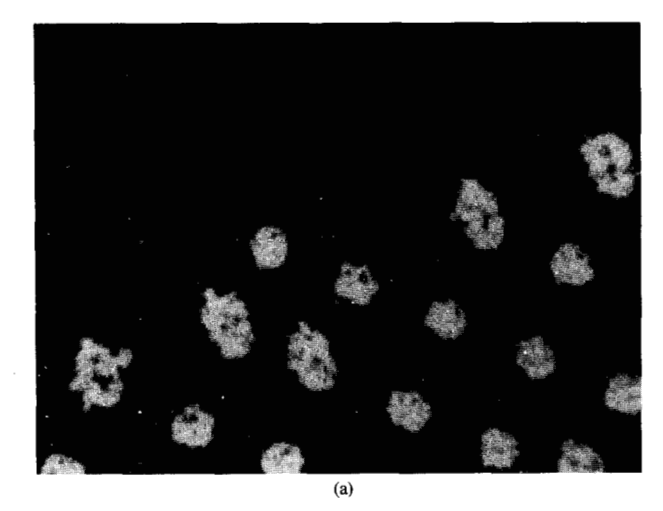
Success in producing good DNP material clearly depends on careful process control of those critical material parameters which determine the functional behavior during end use.

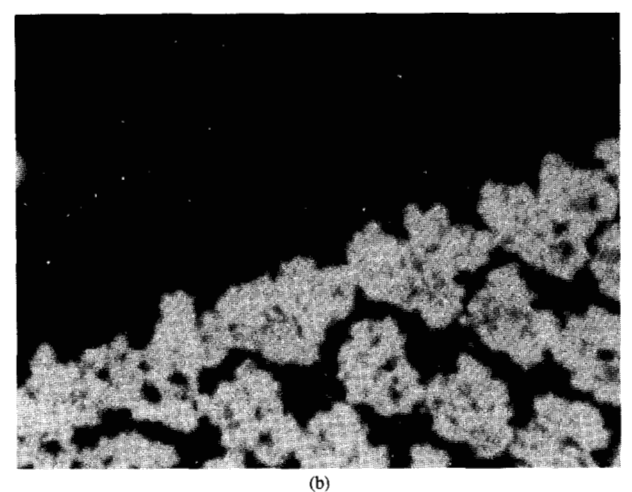
Appendix 1: Role of stylus heating

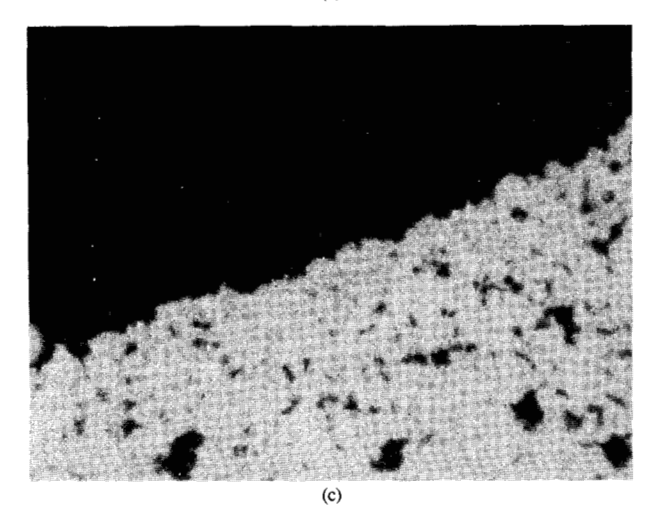
The tungsten styli are heated by the writing process. Special studies described below indicate that when the density of written pels is sufficiently high (high fraction of writing), the consequent elevated temperature of the styli can play an important role in the scratching, head wear, writing, and fouling processes. From these studies it may be inferred that

- 1. Scratching is emphasized at high styli temperatures because of the softening of the polymeric matrix of the underlayer at elevated temperatures.
- Head wear is decreased at high styli temperatures for the same reason, and also because the styli pick up more debris, which acts as an additional lubricant.

¹⁷ The change in R_a and R_z due to calendering increases as the cure temperature is decreased. The temperature and pressure settings of the calender depend on the particular machine used; the correct settings have been used if the R_a and R_z values are reduced by calendering according to the quoted ranges. Temperatures of about 85°C at linear pressures of about 3×10^5 N/m were used for the calender employed in the present experiments.







Transmission optical micrographs showing scratching for special patterns of differing writing fractions. During writing the styli moved diagonally from the lower right to the upper left side of the micrographs. Compared scratching in upper left portions of the micrographs. The writing fraction increases from (a) to (b) to (c).

- 3. Writing quality is adversely affected at high styli temperatures because the enhanced pickup of debris can decrease the writing efficiency.
- Fouling is more pronounced at high styli (and head) temperatures because the softened polymers are more easily picked up and subsequently compacted into a hard cake.

• Scratching

The standard scratch test was routinely carried out in the areas immediately following the large boxes of the pattern of Figure 12 (Section 4). The scratching was most pronounced in such a region, decreasing monotonically with distance from the boundary of the box. The basic reason for this behavior lies in the high temperatures achieved by the styli during the 100% writing of the boxes and the subsequent cooling of the styli upon leaving the boundary of the box.

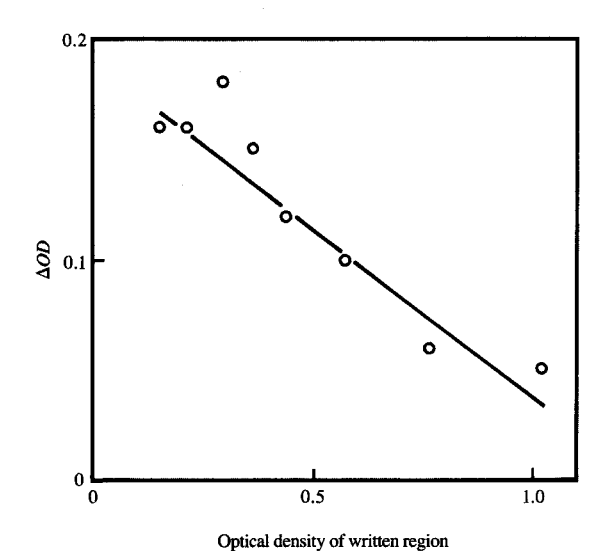
Further support for this view may be found in an experiment where the scratching was studied in regions following special patterns having differing fractions of writing (Figure 18). Here it is seen that the scratching intensified as the written fraction increased. The results are presented in a quantitative manner in Figure 19, which shows that ΔOD , the differential optical density just following the written region, decreased monotonically with increasing optical density of the written region (decreasing fraction of writing). The explanation for this behavior is simply that the increasing written fraction corresponds to higher styli temperatures. In another experiment, a single stylus was moved across a sample of DNP material in a nonfired mode. The stylus was then heated to about 100°C and quickly reinstalled in the apparatus, and the experiment was repeated. The scratching was consistently found to be more pronounced after the stylus was heated.

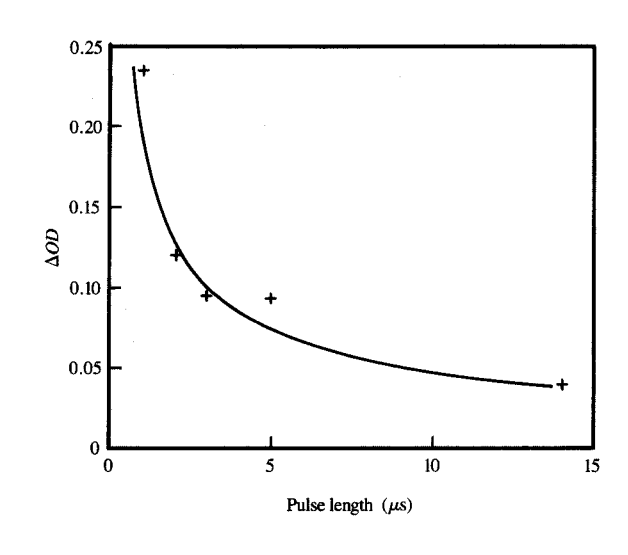
In view of the preceding results, it may be initially surprising that the value of ΔOD following a block of 100% writing decreases rapidly with increasing pulse length, as shown in **Figure 20**. This result becomes understandable when it is realized that debris pickup by the styli is enhanced at long pulse lengths (Section 5), and that the presence of this debris suppresses scratching because of its action as a lubricant (see the following section). Thus, while increased scratching is expected at high styli temperatures, the effect may be partly counterbalanced by enhanced debris pickup under these conditions.

Head wear

In the head wear experiments described in the text, the worst-case condition of 0% writing was used (the head was swept with the writing power off). However, special experiments were also carried out where head wear was monitored for special patterns of written pels having various fractions of writing. ¹⁸ It was found that as the

¹⁸ These experiments were carried out by V. Rudolph of IBM Böblingen.





Transmission optical density change due to scratching, ΔOD , as a function of optical density of a written array of pels. This curve corresponds to the micrographs of Figure 18; the optical density of the array increased with decreasing fraction of writing.

Figure 20

Optical density change due to scratching, ΔOD , as a function of pulse length in region of 100% writing. The region of 100% writing immediately preceded the scratched area.

written fraction increased, the head wear index increased exponentially. The increased stylus temperature associated with increasing written fraction again explains the results; here the softening of the polymeric material with increasing temperature lessens the abrasive action of the underlayer on the styli. Furthermore, under these conditions the styli tips receive a heavier debris deposit, which can act as a lubricant and suppress head wear.

• Writing quality

A rough underlayer is needed to scour debris from the styli tips; the elimination of this debris is important because its presence can lead to deterioration of the writing quality. Under writing conditions leading to high styli temperatures, e.g., long pulse lengths, debris is built up quickly. Worst-case tests for writing thus correspond to conditions where the debris can build up faster than it can be scoured away; such worst-case tests are therefore represented by patterns having high writing fractions, such as those of Figure 18(c), or by an array of fine lines (Section 4).

An illustration of the impact of debris on writing quality is shown in Figure 21, which displays a poor-quality sample. Here a region of 100% writing (top) is followed by an unwritten region (center), which is followed in turn by an area of fractional writing (bottom). It is seen that some

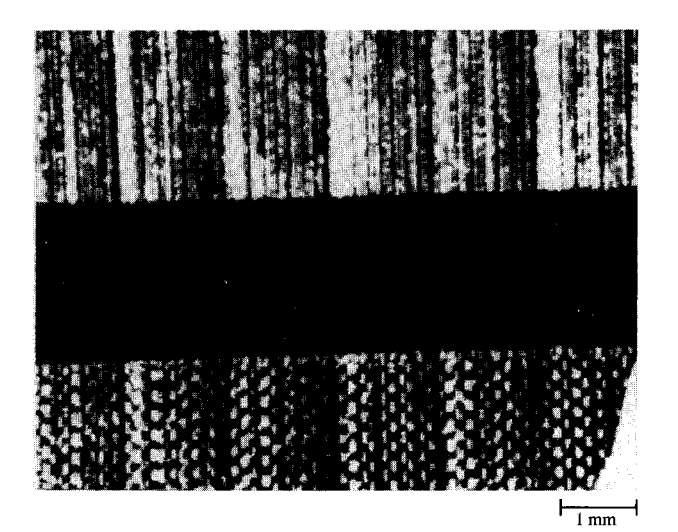


Figure 21

Micrograph of region of 100% writing (top), unwritten region (center), array of written pels (bottom) of a sample showing poor writing. (Writing head moved vertically downward.) Dark bands in top region of 100% writing indicate writing failure caused by pickup of debris by the styli; no scratching is seen in corresponding collinear regions in the center unwritten region. Collinear bands of poor writing continue in bottom region of array of written pels.

509

debris was picked up by the styli in the region of 100% writing (top) as shown by the presence of bands of unwritten material; another set of collinear bands appears in the fractional writing region (bottom), again representing bands of poor writing. In this case a large amount of debris was picked up by the styli, but the scouring action of the underlayer was inadequate to provide sufficient cleaning of the styli even in the intermediate unwritten region.

It is also interesting to note that there was pronounced scratching in the intermediate unwritten region except in the tracks collinear with the unwritten bands, where the scratching was suppressed. Here the accumulated debris acted as a lubricant to inhibit scratching, as noted above.

• Fouling

There is evidence that fouling proceeds faster if polymers having low glass-transition temperatures are employed in the underlayer and/or overlayer. Furthermore, it is known that fouling is accelerated as the percentage of the written area is increased, leading to higher stylus temperatures. The effects of higher stylus temperatures are to increase debris pickup as well as to enhance compaction of debris at the head insulator block.

Appendix 2: Relation between $\triangle OD$ and OD in scratching

When the thickness of the aluminum film (its OD) was decreased, the value of ΔOD , the scratching index, decreased (see third set of entries of Table 5). This result may be explained by postulating that during scratching the areal fraction of totally removed aluminum is *independent* of aluminum thickness. This postulate is consistent with previous studies (Part I) in which scratching was never observed to decrease the thickness of the aluminum in localized regions. Instead, it was found that the aluminum in a scratched area either retained its original thickness or was totally removed in small regions (localized holes) associated with peaks in the underlayer structure.

It then follows that the optical transmission of a scratched area is given by

$$T_{\text{scratch}} = T_{\text{virgin}} + T_{\text{holes}} . \tag{A1}$$

Here $T_{\rm scratch}$ is the net measured transmission in the scratched region, $T_{\rm virgin}$ is the measured transmission in the unscratched (virgin) region, and $T_{\rm holes}$ is the inferred scratched-region transmission which would be measured for an aluminum film thick enough to have a negligible value of $T_{\rm virgin}$; i.e., $T_{\rm holes}$ represents the areal fraction of holes in the aluminum associated with scratching. By definition,

$$\Delta OD = OD_{\text{virgin}} - OD_{\text{scratch}} , \qquad (A2)$$

so that upon noting that $OD = -\log T$, substitution of Equation (A1) into Equation (A2) gives

$$\begin{split} \Delta OD &= -\log T_{\text{virgin}} + \log \left(T_{\text{virgin}} + T_{\text{holes}} \right) \\ &= \log \left(1 + T_{\text{holes}} / T_{\text{virgin}} \right). \end{split} \tag{A3}$$

Following this reasoning, if the aluminum thickness varies among a set of otherwise identical DNP samples, it is expected that $T_{\rm holes}$ would be constant for the set. Then the corresponding values of ΔOD would be predicted by Equation (A3), where for each sample $T_{\rm virgin}=10^{-OD}$, where OD represent the optical density of a virgin region.

From Equation (A3), for a postulated value of T_{holes} of 0.37%, values of ΔOD of about 0.2 and 0.1 are predicted for values of T_{virgin} of 2.18% and 1.88%, respectively, corresponding to the third set of entries of Table 5. The predicted values are close to the given measured values of ΔOD . Measurements of other sets of samples also confirm the model.

Conversely, if the values of OD for a virgin region and ΔOD for a scratched region are known for a given sample, then from Equations (A1) and (A2) the value of T_{holes} is given by

$$T_{\text{holes}} = 10^{-OD} [10^{\Delta OD} - 1].$$
 (A4)

Acknowledgments

J. C. Chen and K. Sachdev made valuable contributions to the chemistry of the DNP materials; T. J. Marsh, J. M. Olson, and K. Presley assisted in the development of the fabrication processes. L. D. Hastings, T. J. Marsh, B. A. Newton, and P. Viscariello helped with the mixing and coating operations. G. Schmidt assisted with materials characterization. Valuable suggestions on organic coating technology and metal-film coating technology were made by D. J. Pipkin and C. R. Guarnieri, respectively. J. Bahr and V. Rudolph developed many of the functional 4250 printer test procedures and carried out many tests. J. M. Karasinski and M. T. Prikas assisted in carrying out many experiments.

Teflon is a registered trademark of E. I. du Pont de Nemours & Co.

References

- T. C. Patton, Paint Flow and Pigment Dispersion, Second Edition, John Wiley & Sons, Inc., New York, 1979.
- 2. D. J. Pipkin, "Method and Apparatus for Forming a Coating on Both Sides of a Substrate," U.S. Patent 4,327,130, 1982.
- "Surface Roughness Terminology—Part 1: Surface and Its Parameters," 4287/1, International Organization for Standardization, Geneva, Switzerland, December 1984.
- "Measuring Particle Sizes," Meas. & Control 2, 142–147 (1963).

Received June 29, 1990; accepted for publication July 25, 1991

Mitchell S. Cohen IBM Research Division, Thomas J. Watson Research Center, P.O. Box 218, Yorktown Heights, New York 10598. Dr. Cohen received his Ph.D. degree from Cornell University, Ithaca, New York. Since joining IBM in 1974, he has worked in the fields of magnetic bubbles and advanced printing technology. Dr. Cohen is currently engaged in research on optoelectronic packaging.

Ali Afzali IBM Research Division, Thomas J. Watson Research Center, P.O. Box 218, Yorktown Heights, New York 10598. Dr. Afzali received his Ph.D. in organic chemistry in 1974 from the University of Pennsylvania, Philadelphia. He was assistant professor of chemistry at Shiraz University, Iran, from 1974 to 1979, and later spent two years in the Department of Chemistry at the University of California, Berkeley, as visiting scholar. In 1981, he joined IBM Research in San Jose, California, as a visiting scientist and worked on lubricants and the lubrication of magnetic disks. In 1983 Dr. Afzali joined the Image Technology group at the Thomas J. Watson Research Center and worked until 1989 on the development of the Direct Plate-Direct Negative. Currently he is a member of a dielectric materials and processes group, working on the development of dielectric composites.

Eva E. Simonyi IBM Research Division, Thomas J. Watson Research Center, P.O. Box 218, Yorktown Heights, New York 10598. Ms. Simonyi is a Senior Research Assistant in the Packaging Department at the Thomas J. Watson Research Center. She received her Master's degree in physics at the Kossuth Lajos Tudomany Egyetem, Debrecen, Hungary, in 1961. Prior to joining IBM she worked at the Belfer Graduate School of Science, New York, where she prepared experiments and conducted studies of the structural properties of magnetite. She is currently involved in studies of the physical properties of polymeric materials. Ms. Simonyi is the recipient of an IBM Invention Achievement Award.

Mukesh Desai IBM General Technology Division, East Fishkill facility, Route 52, Hopewell Junction, New York 12533. Mr. Desai received his B.S. in chemistry from Bombay University, India, and his M.S. in chemistry from Polytechnic University, Brooklyn, New York. He joined the IBM Research Division in 1984 and is currently a staff engineer in the Insulator Process Technology Department in East Fishkill, working on development of chemical-mechanical planarization technology. He holds three U.S. patents and has earned an IBM Invention Achievement Award and an IBM Research Division Award.

Keith S. Pennington IBM Research Division, Thomas J. Watson Research Center, P.O. Box 218, Yorktown Heights, New York 10598. Dr. Pennington graduated with a B.Sc. in physics from Birmingham University, England, in 1957 and a Ph.D. in physics from McMaster University, Hamilton, Ont., Canada, in 1961. He started his research career at Bell Telephone Laboratories, Murray Hill, New Jersey, where he did pioneering work in holography and in particular developed the first multicolor holograms and did early work in holographic interferometry and optical information processing. He joined IBM Research in 1967 and made several leading contributions to the development of improved holographic materials and techniques for three-dimensional scene analysis. Subsequently he initiated the work in and made significant contributions to the development of the Resistive Ribbon Thermal Transfer technology that became the basis for the IBM Quietwriter® printers and other printing programs. Dr. Pennington is Senior Manager of the Image Technologies Department at IBM Research in Yorktown Heights. He currently has responsibility for several image-related research projects in the areas of image compression, document processing, and scanning systems as well as novel highresolution printing processes. In this position he conceived and managed the development of the dual-function electroNEG materials and formulations for directly producing negatives and lithographic printing masters with the IBM 4250 electroerosion printer. He was awarded the Albert Rose Electronic Imager of the Year Award for 1987 by the Institute for Graphic Communications and the 1987 Charles E. Ives Award for Engineering by the Society of Photographic Scientists and Engineers (SPSE). While at IBM, he has received two Outstanding Contribution Awards, two Outstanding Technical Achievement Awards, and an Outstanding Innovation Award. He has also received a Division Level Award and a Corporate Award for his initiation of the Resistive Ribbon Thermal Transfer printing technology. Dr. Pennington is a Fellow of both the Society for Imaging Science and Technology (IST; formerly SPSE) and the Optical Society of America, a Senior Member of the IEEE, and a member of the Society for Information Display (SID). He is also a member of the Editorial Advisory Board of Electronic Imaging.